

Institut für Energie- und Klimaforschung  
Plasmaphysik (IEK-4)

# **Isotope Effects in Molecule Assisted Recombination and Dissociation in Divertor Plasmas**

R. K. Janev, D. Reiter

**Jül-4411**





Institut für Energie- und Klimaforschung  
Plasmaphysik (IEK-4)

# **Isotope Effects in Molecule Assisted Recombination and Dissociation in Divertor Plasmas**

R. K. Janev, D. Reiter

Berichte des Forschungszentrums Jülich  
Jül-4411 · ISSN 0944-2952  
Institut für Energie- und Klimaforschung  
Plasmaphysik (IEK-4)

Vollständig frei verfügbar über das Publikations-  
portal des Forschungszentrums Jülich (JuSER)  
unter [www.fz-juelich.de/zb/openaccess](http://www.fz-juelich.de/zb/openaccess)

Forschungszentrum Jülich GmbH · 52425 Jülich  
Zentralbibliothek, Verlag  
Tel.: 02461 61-5220 · Fax: 02461 61-6103  
[zb-publikation@fz-juelich.de](mailto:zb-publikation@fz-juelich.de)  
[www.fz-juelich.de/zb](http://www.fz-juelich.de/zb)

This is an Open Access publication distributed under the  
terms of the **Creative Commons Attribution License 4.0**,  
which permits unrestricted use, distribution, and



reproduction in any medium, provided the  
original work is properly cited.

# Isotope Effects in Molecule Assisted Recombination and Dissociation in Divertor Plasmas

R.K. Janev<sup>1,2</sup>, D. Reiter<sup>1</sup>

June 5, 2018

## **Abstract**

A burning fusion plasma will necessarily contain a mixture of D and T isotopes, in the atomic, molecular and ionised components. It is demonstrated that molecule assisted recombination (MAR) and dissociation (MAD) mechanisms expected to be strong in typical low-temperature hydrogenic divertor plasmas exhibit a kinetic isotope effect. The effect originates from the mass dependence of rate coefficients of dissociative electron attachment and atomic-to-molecular ion conversion reactions, that are common precursors for MAR and MAD mechanisms.

MAR favours a faster recombination of the lighter ion with plasma electrons, while MAD favours a faster dissociation of the lighter molecule. The effect is cumulative, and during the ion residence time in the divertor it may produce significant differences in the recombined electron-ion pairs of the two isotopes, and in the amounts of dissociation products of the two isotopic molecules. For example a factor of 3 – 9 in MAR, and 22 – 400 in MAD in the concentrations of recombination and dissociation products results, for  $T = 3$  eV,  $n_e = 3 \cdot 10^{14}$  cm<sup>-3</sup> and  $[H_2]:[D_2]:[HD]$  in the range 1:1:0 - 1:1:2. Some implications of MAR and MAD isotope effects for divertor plasma physics are discussed.

---

<sup>1</sup>Institut für Energie- und Klimaforschung, Forschungszentrum Jülich GmbH, Trilateral Euregio Cluster, D-52425 Jülich, Germany

<sup>2</sup>Centre for Energy Research, Macedonian Academy of Sciences and Arts, P.O. Box 428, MK-1000 Skopje, Macedonia

# 1 Introduction

Despite strong frictional forces between the various ionic species present in fusion plasmas, individual isotope flows may still become separated. This is, for example, reflected in a typical explicit mass dependence robustly seen in empirical energy confinement time scalings in tokamaks:  $\tau_E = \tau_E(\dots, A_i)$ , with  $A_i$  denoting the hydrogen isotope mass [1].

The action of particular plasma mirco-instabilities [2], or, notably in the outer plasma (divertor) region, of the mass dependent thermal forces between hydrogenic ion isotopes [3], have been proposed as physical mechanisms quite early.

Even more basic atomic processes, simply due to the mass dependence of hydrogenic atom-ion charge exchange rate coefficients and mean free pathes are clearly present. Such ballistic (cross field) effects from the neutral gas component of the plasma have been proposed as a possible driving mechanism for the observed isotope effects on plasma confinement, as early as 1992 [4].

Isotope separation effects in divertor plasma isotopic ion mixtures related to the presence of hydrogenic molecules, do not seem to have been investigated in the nuclear fusion context. This seems surprising because hydrogenic molecules usually have quite significant concentrations, in particular in so called detached divertor regimes. And furthermore the basic plasma chemical processes have been subject to experimental studies since almost half a century [5].

Recently [6] it was pointed out that different molecular driven volumetric recombination rates may apply in  $H^+$  as compared to  $D^+$  plasmas, solely caused by different thermal ion velocities, at same ion temperatures. But still the identical reaction rates (chemical kinetics) for  $H_2$  and  $D_2$  involving processes, just scaled to same thermal velocities, have been applied.

The purpose of the present work it to consider isotope separation (isotope conversion) effects (“forces”) in an isotopic divertor plasma mixture, which are chemical in nature, i.e., driven by the molecular structure itself. In a (detached) fusion divertor plasma these chemical kinetics effects might act on top of the mentioned plasma collisionality driven thermal forces.

## 1 Introduction

---

The issue of enrichment of one ionic species relative to another near neutraliser plates is not only important for helium ash removal from a burning D-T plasma, but also for the critical divertor design issue of tritium cycle and retention. In the present paper we discuss an additional physical mechanism, which may lead to separation of the various hydrogenic isotopes, e.g. of D and T ions, in particular in the favorable low temperature high density divertor conditions. This mechanism is a direct consequence of (vibrationally excited) molecules and their influence on the momentum balance, and, hence, on divertor plasma dynamics in general.

A change in chemical reaction rate, when in a molecule one isotope is exchanged with another, results from heavier isotopologues having a lower velocity/mobility (at a given temperature) and also a modified stability against dissociation when compared to the compounds containing other isotopes. Isotopic effects on rate coefficient are typically strongest when the change in the relative mass is greatest, in particular when the effect is related to vibrational frequencies of the affected bonds. In a fusion divertor plasma containing H and D ions, changing a hydrogen atom (H) to its isotope deuterium (D) represents a 100% increase in mass. Even if the potential energy surface for a reaction is nearly identical, heavier isotopes (classically) lead to lower vibration frequencies, or, viewed quantum mechanically, will have lower zero-point energy and a narrower spacing of vibrational eigen-states.

The earlier anticipated important role of collision processes involving vibrationally excited molecules in low temperature (1–10 eV) fusion divertor plasmas [7] has later been demonstrated in so-called molecule assisted recombination (MAR) [8, 9] and (by abuse of language) molecule assisted dissociation (MAD) [10] in such plasmas.

As we will argue in the present paper, in a quasi-stationary H/D plasma of temperatures 1–3 eV and densities below  $\sim 5 \cdot 10^{14} \text{ cm}^{-3}$  the isotope effect per MAR/MAD reaction time  $\tau_c$  in MAR is in the range of 1% - 4% and that in MAD in the range of 2% - 14%, depending on the ratio  $[\text{H}_2]:[\text{D}_2]:[\text{HD}]$  of neutral molecule concentrations. For an ion residence time in the divertor  $\tau_t \gg \tau_c$  this may lead to amplification of the single step isotope effect to observable isotope separation factors of order 10, in a sense further specified below.

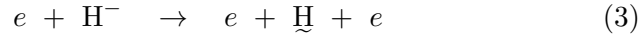
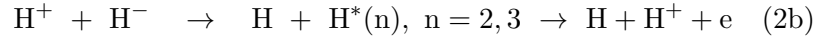
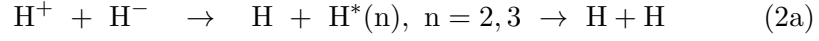
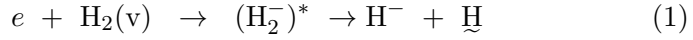


## 1 Introduction

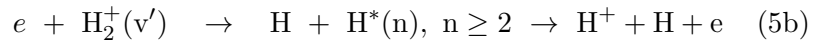
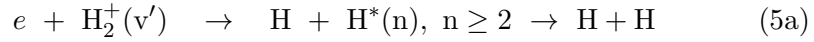
---

The MAR and MAD mechanisms are mutually inter-related and, in the plasma temperature region below  $\sim 5$  eV, both proceed via similar electron and ion collision chain reactions. For a single isotope hydrogenic plasma (now H being used as placeholder for H, D or T isotopes), these reaction chains are:

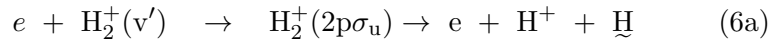
(i): Negative ion (NI) mediated MAR and MAD channels:



(ii): Ion conversion (IC) MAR and MAD channels:



as well as the direct dissociative excitation of  $\text{H}_2^+(\text{v}')$ , which proceeds either via the intermediate excited  $\text{H}_2^+(2\text{p}\sigma_{\text{u}})$  state or via indirect processes involving energetically high lying auto-ionising states  $\text{H}_2^{**}$  or  $\text{H}_2^{*\text{Ryd}}$  of the neutral molecule:



The reaction chains  $(1 \rightarrow 2\text{a})$  and  $(4 \rightarrow 5\text{a})$  constitute the NI [7] and IC [8] recombination channels, respectively, while the reaction chains  $(1 \rightarrow (2\text{b}))$  and  $(4) \rightarrow [5\text{b} \text{ or } 6])$  constitute the NI and IC dissociation channels

## 1 Introduction

---

[10], respectively. Reaction chain  $(1 \rightarrow 3)$  just provides an additional indirect channel to the ordinary electron impact molecule dissociation reaction, albeit with distinct reaction energy kinetics.  $(\text{H}_2^-)^*$  in Eq. (1) is an unstable intermediate (resonant) state of the  $(e, \text{H}_2)$  system.  $\text{H}^*(n)$  in Eqs. (2) and (5) is an excited H-atom on the energy level with principal quantum number  $n$ , and  $v$  ( $v'$ ) in  $\text{H}_2(v)$  ( $\text{H}_2^+(v')$ ) is the quantum number of the vibrational level of the excited molecule (molecular ion).  $\text{H}$  and  $\underline{\text{H}}$  in Eqs. (1)–(6) are ground-state hydrogen atoms.

In the NI and IC MAR processes a plasma electron-ion pair is recombined and a  $\text{H}_2(v)$  molecule is dissociated to the “new-born”  $\text{H}$  and  $\text{H}^*(n)$  neutral atoms. In the NI and IC MAD processes only dissociation of a  $\text{H}_2(v)$  takes place producing two “new-born” ground state atoms  $\text{H}$ .

We point out a frequently encountered pitfall when these processes have been discussed without further specifications. There is a certain ambiguity regarding the notations MAR and MAD in the literature. When the “true” volumetric recombination rates and the dissociation degree are discussed (e.g. for parallel plasma momentum removal from the parallel ion flow in the divertor), then only the narrower definition of MAR, i.e. only final channel steps (2a) and (5a) are counted. The final channel steps (2b) and (5b) are then referred to as contributions to MAD.

When the precursor steps are in the focus of a discussion, as it is the case in the present work on isotope separation, or, e.g. on molecular contributions to hydrogenic line emissions from the divertor, then the wider definitions of MAR and MAD are often used, in which *both* final channel steps in (2) and in (5) are counted as “MAR”. Depending on plasma density and temperature these two definitions of MAR and MAD may differ by more than an order of magnitude [15]. In the present work we use the latter (wider) definition of MAR, and discuss the direct products of the precursor steps  $\text{H}^*(n)$  (MAR) and  $\underline{\text{H}}$  (MAD). I.e. in this notation we count far more processes as MAR, at the expense of those counted as MAD.

We see that Eq. (1) serves as a common precursor for the MAR and MAD NI mediated channels, whereas Eq. (4) plays the same role for the IC MAR and MAD channels. We also see that reactions (2a) and (2b), completing the NI MAR and NI MAD mechanisms, respectively, are mutually competing

## 1 Introduction

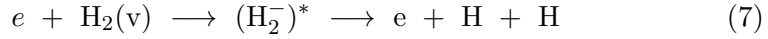
---

processes. The rate coefficients  $K_{2a}$  and  $K_{2b}$  of these two reactions become equal at  $T \simeq 1.5$  eV [11] with  $K_{2a} > K_{2b}$  for  $T < 1.5$  eV, and *vice versa*. Reactions (5a) and (5b+6a), completing the IC MAR and IC MAD channels, are also mutually competing, and have equal rate coefficients again at  $T \simeq 1.5$  eV, with  $K_{5a} > K_{5b+6a}$  for  $T < 1.5$  eV [11].

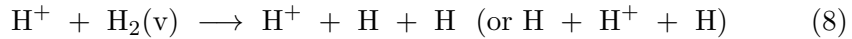
The indirect dissociative excitation channel (6b), which was not yet accounted for in [11], is large at low  $T$  (below 1–2 eV) and may change this situation in favour of IC MAD.

The  $H^*(n)$  product of NI and IC MAR processes can be destroyed either by electron-impact ionization (directly, or via up-ward cascading, completing the reaction chains (2b) and (5b)) or by collision-radiative decay (directly radiative, or via down-ward electron-impact or radiative cascading, as in reaction chains (2a) and (5a)) to the ground state. Only the latter of these process chains leads to recombination (and completes the mechanism). The  $\underline{H}$  product of MAD processes is the end product of this mechanism; its destruction by electron-impact ionization in a stationary bath of  $H_2$  molecules indicates the beginning of a new cycle of operation of this mechanism.

It should be also mentioned that the “direct” reactions



with both H atoms in the ground state, and (“direct proton-impact dissociation”)



give negligibly small contributions to, respectively, the ordinary electron impact molecule dissociation reaction and the IC MAD channel at all temperatures [11, 12, 13].

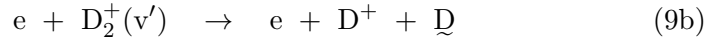
It should be emphasized that the above given definitions of MAR and MAD mechanisms reflect their mutually competing role in the destruction of channel mediating particles,  $H^-$  and  $H_2^+(v')$ . However, as Eqs. (1), (2a) and (4), (5a), respectively, indicate, besides producing a recombined electron-ion pair, the MAR mechanism also leads to dissociation of the initial molecule. Therefore, the total molecular dissociation degree in the considered plasma

## 1 Introduction

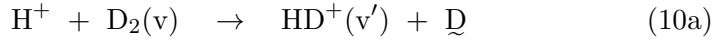
---

temperature region results from both MAR and MAD, as well as from direct processes.

Another molecule assisted dissociation mechanism, which occurs in a two isotope plasma (say: H/D plasma) is related to isotopic reaction asymmetry. Examples of this type of MAD (precursors) are:

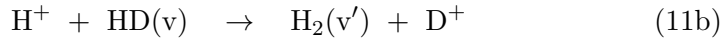
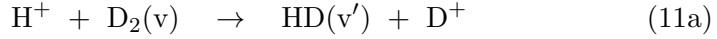


and



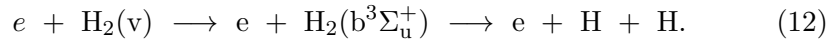
The effect of these reaction chains is equivalent to the (direct) dissociation charge exchange (CX) reaction  $\text{H}^+ + \text{D}_2(\text{v}) \rightarrow \text{H} + \text{D} + \text{D}^+$ . We shall call this dissociation mechanism CX-MAD. A specific feature of CX-MAD is that it leads to ion isotope conversion:  $\text{H}^+ \rightarrow \text{D}^+$  (in the above reactions) and  $\text{D}^+ \rightarrow \text{H}^+$  (in the similar reactions for the  $\text{D}^+ + \text{H}_2(\text{v})$  system).

The particle rearrangement (isotope exchange) reactions, such as



also lead (directly) to isotope ion conversion.

The importance of MAR and MAD mechanisms in divertor plasmas stems from the facts that at plasma densities below  $\sim 5 \times 10^{14} \text{ cm}^{-3}$  and temperatures above  $\sim 0.5 \text{ eV}$ , the rates coefficients of conventional radiative and three-body recombination mechanisms appear to be smaller than those of MAR [8]. This translates to the corresponding collision rates, for similar electron and molecule densities, i.e., unless specific plasma and neutral transport processes change the situation, see e.g. [14]). And for temperatures below 4-5 eV the rate coefficients of MAD are significantly larger than those for the direct electron impact dissociation of  $\text{H}_2(\text{v})$  proceeding via excitation of the  $\text{H}_2(b^3\Sigma_u^+)$  repulsive state, [11].



## 1 Introduction

---

Regarding the relative importance of MAR and MAD processes, calculations within a collisional-radiative model show [10, 15] that for plasma electron densities below  $\sim 5 \times 10^{14} \text{ cm}^{-3}$  the MAD process dominates for  $T \gtrsim 1 \text{ eV}$ , while for  $0.5 < T < 1 \text{ eV}$  MAR is dominant, at least as long as the indirect dissociation excitation channel Eq. (6b) is not too large.

In the present work we shall study the MAR and MAD kinetics for a two-isotope divertor plasma in the plasma parameter region  $n_e \lesssim 5 \times 10^{14} \text{ cm}^{-3}$ ,  $T \lesssim 4 - 5 \text{ eV}$  (in which these mechanisms are most efficient). The study will be focused on the question of existence of an isotopic effect in overall MAR and MAD (i.e. after averaging over the populations of vibrational levels in reactions (1) and (4)). Namely, it is well known (both experimentally [16, 17] and theoretically [18, 19, 20]) that the dissociative attachment (DA) reaction (1) exhibits a pronounced isotope effect (e.g.  $\sigma_{\text{H}_2}^{\text{DA}}(v=0)$  is 200 [16] to 400 [12] times larger than  $\sigma_{\text{D}_2}^{\text{DA}}(v=0)$  at the reaction energy threshold) which, however, decreases with increasing the vibrational level  $v$ , and diminishes when  $v$  approaches the dissociation limit [12, 20]. On the other hand, the cross section  $\sigma^{\text{DA}}(v)$  has a very strong dependence on vibration state  $v$  (e.g. at the threshold  $\sigma_{\text{H}_2}^{\text{DA}}(v=0) \approx 10^{-21} \text{ cm}^2$ , whereas  $\sigma_{\text{H}_2}^{\text{DA}}(v=5) \simeq 10^{-16} \text{ cm}^2$ ) and the dominant contribution to the NI MAR and MAD processes comes from the high- $v$  levels (for which, however, the isotope effect in DA is less expressed).

The cross section  $\sigma^{\text{CI}}$  of ion-conversion reaction (4) at low collision energies ( $E \lesssim 5 \text{ eV}$ ) contains contributions from the pure electron capture (or charge exchange) process,  $\sigma^{\text{CX}}$ , as well as from particle exchange (or atom rearrangement) process,  $\sigma^{\text{PX}}$ , both of which exhibit strong dependence on vibrational excitation of  $\text{H}_2(v)$  [13, 21]. The cross section for particle exchange  $\sigma^{\text{PX}}$  shows also a mass dependence [13]. (According to the Langevin model of ion-conversion reactions in the thermal energy region,  $\sigma^{\text{CI}} \sim \mu^{-\frac{1}{2}}$ , where  $\mu$  is the reduced mass of ion-molecule system [22].)

The existence of an isotope effect in MAR and MAD mechanisms after averaging over vibrational level populations of isotopic molecules, would have important implications for plasma and neutral particle transport, hydrogen isotope recycling and inventory in plasma facing materials, and for the particle exhaust from the divertor. Obviously, the MAR isotope effect

## 2.1 Plasma conditions and atomic/molecular processes

---

would act (together with the CX-MAD and reactions of the type (11)) as an ion-charge separation mechanism, while the MAD isotope effect would act as a neutral particle momentum separation mechanism. Indeed, in dissociative processes, such as (1), (5) and (6), the total energy shared by dissociation products is isotope invariant (being determined by the potential energy of dissociating state above the dissociation limit, i.e. by the molecular electronic structure only), while the velocities of dissociation products are inversely proportional to the square roots of their masses. (In symmetric diatomic systems, such as  $H_2$  and  $D_2$ , the dissociation products share the total released energy equally.) The mean values of total kinetic energies released (KER) in the products from reactions (1), (5) (taken at the center of the Franck-Condon region) are 6.74 eV,  $(E_{el} + 13.6/n^2)$  eV, respectively, and, in the direct dissociative excitation channel (6a): 8.6 eV [11], where  $E_{el}$  is the energy of the incident electron in process (5), with mean value  $\bar{E}_{el} \approx 0.88T_e$ .

The organization of our paper is as follows. In the next section we formulate the problem in terms of kinetic rate equations and introduce the simplifying assumptions for its solution. In Section 3 we derive the relative ion and atom isotope enhancement factors for MAR and MAD, and in Section 4 we estimate these relative isotope enrichments during ion residence time in divertor region. The effects of MAR, CX-MAD and direct isotopic ion conversion reaction of type 11 on the isotope ion charge separation are discussed in Section 5. In Section 6 we give some concluding remarks.

## 2 Formulation of the problem and MAR/MAD kinetics

### 2.1 Plasma conditions and atomic/molecular processes

We consider typical conditions in a low-temperature ( $0.5 \text{ eV} \lesssim T \lesssim 3\text{-}4 \text{ eV}$ ) quasi-stationary H/D (detached) divertor plasma also containing a mix of  $H_2$ ,  $D_2$  and HD molecules and plasma densities  $[e]$  ( $= [H^+] + [D^+]$ ) below  $\sim 5 \times 10^{14} \text{ cm}^{-3}$ . HD molecules are formed by isotope exchange reactions in plasma volume, and (more efficiently) by wall processes during the recycling.

## 2.1 Plasma conditions and atomic/molecular processes

---

We shall confine our study to the initial stage of operation of MAR and MAD mechanisms when the concentrations  $[H^*]$ ,  $[D^*]$ ,  $[H]$ ,  $[D]$  of MAR and MAD products are much smaller than the concentrations of “reservoir” particles ( $[H_2]$ ,  $[D_2]$ ,  $[HD]$ ,  $[H]$ ,  $[D]$ ,  $[H^+]=[D^+]=[e]/2$ ). While the plasma and neutral particle transport effects are neglected in the present study, the finite residence time of plasma ions in the divertor will be taken into account when estimating the total MAR and MAD isotope effects (Sections 4).

For the considered H/D plasma conditions and composition the H ( $H_2$ ) NI and IC MAR and MAD reactions (1)-(6) are paralleled by similar reactions for D ( $D_2$ ), as well as by similar molecular processes involving HD. The most important processes contributing to MAR and MAD kinetics in the considered range of plasma parameters are given in Table 1. (On the basis of available information of reaction rate coefficients [11, 23, 24], processes of the type (7) and (8), or ion-molecule reactions involving formation and destruction of three-atomic molecular ions, such as  $H_3^+$ ,  $H_2D^+$ , etc., are considered of lesser importance for MAR/MAD kinetics in the studied range of plasma parameters and are not included in Table 1.) It is also assumed that molecular species involved in the reactions of Table 1 are vibrationally excited according to a certain vibrational level distribution.

With respect to the reactions in Table 1 we make the following remarks. The presence of HD molecules in the plasma contributes significantly to the complexity of MAR and MAD kinetics. The processes involving formation and destruction of HD (such as the isotope exchange reactions, 20–23 and 30–33 in Table 1, for instance) obviously couple the kinetics of individual isotopes, and, therefore, tend to smear out the isotopic effects of MAR and MAD mechanisms. Even in absence of HD molecules, the “cross-symmetric” charge exchange reactions 5 and 6 in Table 1 mix the NI MAR channels for H and D, and, as we shall see later, introduce a complete isotope symmetry in the overall NI MAR mechanism (thus excluding in principle the possibility of an isotope effect in NI MAR). This isotopic symmetry of the NI MAR kinetics is not broken even in presence of HD molecules in the plasma. In the case of IC MAR and NI/IC MAD mechanisms, partial isotopic symmetry appears only in presence of HD molecules (via the reactions 13, 26 and 29 in Table 1). Therefore, the intrinsic isotopic reaction asymmetry of IC

## 2.1 Plasma conditions and atomic/molecular processes

---

MAR and NI/IC MAD channel kinetics should, in principle, generate isotope effects in MAR and MAD in a two-isotope plasma. We further note that reactions 20 and 22 in Table 1, and their respective inverse reactions 32 and 30, convert the reservoir particles into each other and do not participate in MAR and MAD reaction kinetics. (Only when  $[\text{HD}] \ll [\text{H}_2], [\text{D}_2]$ , they become relevant.)

These reactions, however, are important as direct ion charge conversion mechanisms (see Section 5).

It is important to note that in the considered plasma temperature region ( $T \lesssim 4\text{--}5$  eV), the excited  $\text{H}^*(n)$  and  $\text{D}^*(n)$  atoms produced in mutual neutralisation reactions 2 and 4 of Table 1, respectively, are predominantly in  $n = 3$  state, while those produced in dissociative recombination reactions 15, 17 and 26 of Table 1 are predominantly in  $n = 2, 3, 4$  and 5 states (with population weights  $g_2=0.10$ ,  $g_3=0.45$ ,  $g_4=0.22$  and  $g_5=0.12$ , respectively, [11]). Reactions 34–37 in Table 1 provide a coupling of the  $n - n'$  states within a given atomic isotope, while reactions 9 and 10 provide an  $n - n'$  coupling between the excited states of the two atomic isotopes (except in the resonant case  $n' = n$ ). This latter  $n - n'$  coupling makes the rate equations for  $\text{H}^*(n)$  and  $\text{D}^*(n')$  also coupled (and thereby introduce a non-linearity in the problem). However, for plasma densities below  $\sim 5 \times 10^{14} \text{ cm}^{-3}$  and  $T \lesssim 4\text{--}5$  eV, the radiative lifetimes of  $n = 2, 3$  levels are still considerably shorter than the collisional times for the  $n - n'$  processes ( $n' \neq n$ ) in reactions 9, 10, 36, 37. Therefore, the MAR kinetics can be reduced to that of  $\text{H}^*(n = 3)$  and  $\text{D}^*(n = 3)$  atomic products only, assigning an effective population weight of  $n = 3$  level in reactions 15, 17 and 26 (e.g.,  $\bar{g} \simeq g_2 + g_3 + g_4 \simeq 0.8$ ). In a more accurate treatment, the effects of reactions 34 – 37 on the effective population of  $n = 3$  level can be included by solving a “restricted” collisional-radiative model for the  $\text{H}^*$  and  $\text{D}^*$  products produced from mutual neutralisation or dissociative recombination. We mention that the  $n - n'$  isotope coupling does not exist in the MAD kinetics.

According to presently available cross section (or rate coefficients) information on the reactions included in Table 1 [11, 12, 13, 21, 23, 24, 25, 26], and also for those involving vibrationally excited molecular species, one can make the following comments:



## 2.2 Rate equations for MAR kinetics

---

(I) In the temperature region below 3-4 eV, the rate coefficients  $K_j$  of reactions in Table 1 obey the relations:

$$K_2 = K_4 = K_5 = K_6,$$

$$K_7 = K_8, K_9 = K_{10}, (K_{7,8} \gg K_{9,10}, n \neq n'),$$

$$K_{13a} = K_{13b} = K_{13}/2,$$

$$K_{24} = K_{25},$$

$$K_{26a} = K_{26b} = K_{26}/2,$$

$$K_{29a} = K_{29b} = K_{29}/2,$$

$$K_{15} \simeq K_{17} \simeq K_{26},$$

$$K_{27} \simeq K_{28} \simeq K_{29},$$

$$K_{21}, K_{23} \ll K_{24}, K_{26}, K_{29},$$

$$K_{38} = K_{39},$$

$$K_{31}, K_{33} \ll K_{14}, K_{16};$$

(II) Reactions involving  $H_2^+$ ,  $D_2^+$ ,  $HD^+$  + H, D collisions (e.g. reactions inverse to 14, 16, 18, 19, etc.) can be neglected with respect to dissociative recombination reactions of these ions with electrons;

(III) Reactions 21, 23, 31, 33 are strongly endothermic (they become exothermic only for  $v \gtrsim 5 - 6$ ) and can be neglected in the kinetics.

## 2.2 Rate equations for MAR kinetics

In MAR kinetics we are primarily interested in the variation of concentrations of  $H^*$  and  $D^*$  atoms (we drop the label  $n$  or  $n = 3$  for brevity). Taking into account the discussion in the preceding sub-section, the comments (I)-(III) above, and that  $[H^+] = [D^+] = [e]/2$ , the rate equations for the MAR kinetics can be written in the form

$$\begin{aligned} \frac{d[H^*]}{dt} &= \frac{1}{2} K_2 [e] ([H^-] + [D^-]) + K_{15} [e] [H_2^+] + K_{26a} [e] [HD^+] \\ &\quad - (K_7 [e] + A_3) [H^*] \end{aligned} \quad (13)$$

$$\begin{aligned} \frac{d[D^*]}{dt} &= \frac{1}{2} K_2 [e] ([H^-] + [D^-]) + K_{17} [e] [D_2^+] + K_{26b} [e] [HD^+] \\ &\quad - (K_8 [e] + A_3) [D^*] \end{aligned} \quad (14)$$

## 2.2 Rate equations for MAR kinetics

---

and

$$\frac{d[\text{H}^-]}{dt} = K_1[e][\text{H}_2] + K_{13a}[e][\text{HD}] - (K_2 + K_{11})[e][\text{H}^-] \quad (15)$$

$$\frac{d[\text{D}^-]}{dt} = K_3[e][\text{D}_2] + K_{13b}[e][\text{HD}] - (K_2 + K_{11})[e][\text{D}^-] \quad (16)$$

$$\frac{d[\text{H}_2^+]}{dt} = \frac{1}{2}(K_{14} + K_{19})[e][\text{H}_2] - (K_{15} + K_{27})[e][\text{H}_2^+] \quad (17)$$

$$\frac{d[\text{D}_2^+]}{dt} = \frac{1}{2}(K_{16} + K_{18})[e][\text{D}_2] - (K_{17} + K_{28})[e][\text{D}_2^+] \quad (18)$$

$$\frac{d[\text{HD}^+]}{dt} = K_{24}[e][\text{HD}] - (K_{26} + K_{29})[e][\text{HD}^+] \quad (19)$$

where  $A_3$  in Eqs. (13) and (14) is the total radiative decay rate of the  $n = 3$  hydrogen level. Eqs. (13), (14) are written for the  $\text{H}^*(n=3)$  and  $\text{D}^*(n=3)$  atoms. In order to obtain the recombined electron-ion pairs in the ground states of H and D, the solutions for  $[\text{H}^*]$  and  $[\text{D}^*]$  of Eqs. (13), (14) should be multiplied by the branching ratio  $A_3/(K_7[e] + A_3)$ .

Due to the block structure of the coefficient matrix of the system of equations (13) – (19) one can first solve Eqs. (15) – (19), and then, from this solution, find the solution of Eqs. (13), (14).

It is assumed that molecular species in Eqs. (13)–(19) are all vibrationally excited, but the corresponding vibrational labels  $v$  and  $v'$  in these equations have been omitted. With this in mind, Eqs. (13)–(19), in fact, represent a large system of  $v - v'$  coupled equations.

The vibrational decoupling of this system of equations can be achieved (approximately) by taking into account that electron-impact inelastic processes involved in Eqs. (13)–(19) depend dominantly on the transition energy (determined by the electronic structure of the molecule or molecular ion, that is the same for all hydrogen isotopomers). Consequently, one can introduce an “equivalency” of vibrational levels in different isotopic molecular species by the equality of transition energy for a specific process (or, equivalently, by the equality of their vibrational energy) [27].

Using this “equivalent level” approximation and summing Eqs. (17)–(19) over the populations of  $v'$  levels of molecular ions for each  $v$ -level of neutral molecules, the system (13)–(19) becomes vibrationally decoupled, but still holds for any of the (equivalent) vibrational levels  $v$  of  $\text{H}_2$ ,  $\text{D}_2$  and  $\text{HD}$  (the label of which is still omitted in (13)–(19)).

## 2.2 Rate equations for MAR kinetics

---

Equations (15)–(19) all have the form

$$\frac{d[y]}{dt} = K_0[AB] - \kappa[y] \quad (20)$$

with  $K_0$  and  $\kappa$  being the total production from the external “reservoir” components, and destruction rates of particle  $y$ , respectively. The solution of Eq. (20) with the initial condition  $[y(0)]=0$  is

$$[y] = \frac{K_0[AB]}{\kappa} (1 - e^{-\kappa t}). \quad (21)$$

The total destruction rate  $\kappa$ , thus, determines the timescale  $\tau$  ( $\sim 1/\kappa$ ) on which  $[y]$  attains its equilibrium value  $[y]_\infty = K_0[AB]/\kappa$ . From Eqs. (21) and (15,16) we see that the characteristic times for approach to equilibrium for  $[H^-]$  and  $[D^-]$  are the same,  $\tau_{H^-} = \tau_{D^-} = 1/(K_2 + K_{11})[e]$ .

Since on theoretical grounds, isotope effects are not expected in dissociative recombination (reactions 15, 17, 26) and dissociative excitation (reactions 27, 28, 29) of hydrogenic molecular ions (confirmed also by detailed calculations, [26]), we have  $K_{15} \simeq K_{17} \simeq K_{26}$  and  $K_{27} \simeq K_{28} \simeq K_{29}$  for the energetically “equivalent” vibrational levels of  $H_2^+$ ,  $D_2^+$  and  $HD^+$ . Therefore, characteristic equilibrium times for  $[H_2^+]$ ,  $[D_2^+]$  and  $[HD^+]$  are the same,  $\tau_{H_2^+} = \tau_{D_2^+} = \tau_{HD^+} = 1/(K_{15} + K_{27})[e]$ .

For  $[e]=10^{14} \text{ cm}^{-3}$  and  $T=1, 2$  and  $3 \text{ eV}$ , the values of  $\tau_{H^-}$  are  $1.4 \times 10^{-7} \text{ s}$ ,  $0.83 \times 10^{-7} \text{ s}$  and  $0.54 \times 10^{-7} \text{ s}$ , respectively. After averaging  $K_{15}$  and  $K_{17}$  over the vibrational distribution of  $H_2^+$  [11], the values of  $\tau_{H_2^+}$  for the same plasma density and temperatures are  $1.35 \times 10^{-7} \text{ s}$ ,  $1.11 \times 10^{-7} \text{ s}$  and  $0.91 \times 10^{-7} \text{ s}$ , respectively.

Upon introduction of solutions (21) of Eqs. (15)–(19) into Eqs. (13) and (14), the time evolution of concentrations  $[H^*]$  and  $[D^*]$  becomes dependent on  $\tau_{H^-}$  and  $\tau_{H_2^+}$  as well. However, in Eqs. (13), (14) there is also another characteristic timescale defined by destruction processes of  $H^*$  and  $D^*$  in the  $n = 3$  level, i.e.  $\tau_{H^*} = \tau_{D^*} = 1/(K_7[e] + A_3)$ . For  $[e]=10^{14} \text{ cm}^{-3}$  and  $T=1, 2$  and  $3 \text{ eV}$ , the values of  $\tau_{H^*}$  are [11]:  $0.46 \times 10^{-8} \text{ s}$ ,  $0.42 \times 10^{-8} \text{ s}$  and  $0.40 \times 10^{-8} \text{ s}$ , respectively. For these plasma parameters  $\tau_{H^*}$ ,  $\tau_{D^*}$  are more than an order of magnitude smaller than  $\tau_{H^-}$  and  $\tau_{H_2^+}$ . The strong inequality of  $\tau_{H^*}$  and  $\tau_{H^-}$  ( $\tau_{H_2^+}$ ) remains up to  $[e] \simeq 5 \times 10^{14} \text{ cm}^{-3}$ . This indicates that

## 2.2 Rate equations for MAR kinetics

---

the time evolution of  $[H^*]$  and  $[D^*]$  is determined by  $\tau_{H^-}$  and  $\tau_{H_2^+}$  only, i.e. by the timescale of  $[H^*]$ ,  $[D^*]$  production processes. Neglecting, therefore, the last terms in Eqs. (13) and (14), the production rates for  $[H^*]$  and  $[D^*]$  become

$$\begin{aligned} \frac{d[H^*]}{dt} &= \frac{[e]}{2} \chi_1 (K_1[H_2] + K_3[D_2] + K_{13}[HD]) (1 - e^{-t/\tau_{H^-}}) \\ &+ \frac{[e]}{2} (\chi_2 K_{24}[HD] + \chi_3 (K_{14} + K_{19})[H_2]) (1 - e^{-t/\tau_{H_2^+}}) \end{aligned} \quad (22)$$

$$\begin{aligned} \frac{d[D^*]}{dt} &= \frac{[e]}{2} \chi_1 (K_1[H_2] + K_3[D_2] + K_{13}[HD]) (1 - e^{-t/\tau_{H^-}}) \\ &+ \frac{[e]}{2} (\chi_2 K_{24}[HD] + \chi_3 (K_{16} + K_{18})[D_2]) (1 - e^{-t/\tau_{H_2^+}}), \end{aligned} \quad (23)$$

where

$$\chi_1 = \frac{K_2}{K_2 + K_{11}}, \quad \chi_2 = \frac{K_{26}}{K_{26} + K_{29}}, \quad \chi_3 = \frac{K_{15}}{K_{15} + K_{27}} \quad (24)$$

The coefficients  $\chi_i$  are branching ratios for the MAR channel reactions with respect to competing MAD reactions.

We mention that Eqs. (22) and (23) are valid for all vibrational levels of  $H_2$ ,  $D_2$  and  $HD$  (the label  $v$  is still omitted), but the quantities  $\chi_i$ ,  $\tau_{H^-}$  and  $\tau_{H_2^+}$  do not depend on molecular  $v$ -levels. Equations (22) and (23) have simple solutions of the form

$$[y^*] = K_{H^-} \left( t + \tau_{H^-} e^{-t/\tau_{H^-}} \right) + K_{H_2^+} \left( t + \tau_{H_2^+} e^{-t/\tau_{H_2^+}} \right) \quad (25)$$

where  $K_{H^-}$  and  $K_{H_2^+}$  are the terms in front of the expressions  $[1 - \exp(-t/\tau)]$  in Eqs. (22) and (23), respectively.

As a measure for the isotope effect in  $[H^*]$  and  $[D^*]$  production one can take the ratio  $R_{H/D}^{MAR} = [H^*]/[D^*]$  at times considerably larger than  $\tau_{H^-}$  and  $\tau_{H_2^+}$ . From Eqs. (25), (22), (23) one then obtains (we now write the label  $v$  for the vibrational levels in molecules)

$$\begin{aligned} R_{H/D,v}^{MAR} &= \left( \chi_1 (K_{1,v}[H_2]_v + K_{3,v}[D_2]_v + K_{13,v}[HD]_v) \right. \\ &\quad \left. + \chi_2 K_{24,v}[HD]_v + \chi_3 (K_{14,v} + K_{19,v})[H_2]_v \right) \\ &\quad / \left( \chi_1 (K_{1,v}[H_2]_v + K_{3,v}[D_2]_v + K_{13,v}[HD]_v) \right. \\ &\quad \left. + \chi_2 K_{24,v}[HD]_v + \chi_3 (K_{16,v} + K_{18,v})[D_2]_v \right) \end{aligned} \quad (26)$$

### 2.3 Rate equations for MAD kinetics

---

The summation of  $R_{\text{H/D},v}^{MAR}$  over vibrational level populations in  $\text{H}_2$ ,  $\text{D}_2$  and  $\text{HD}$  will be discussed in the next Section. We mention again that in order to obtain the number of recombined electron-ion pairs,  $[\text{H}^*]_{1s}$  and  $[\text{D}^*]_{1s}$ , one has to multiply  $[\text{H}^*]$ ,  $[\text{D}^*]$ , given by Eq. (25), by  $A_3/(K_7[e] + A_3)$ . This factor however does not affect the ratio  $R_{\text{H/D},v}^{MAR}$ .

### 2.3 Rate equations for MAD kinetics

In MAD kinetics we are primarily interested in the variation of concentrations of  $\text{H}$  and  $\text{D}$  atoms. Keeping in mind the remarks (I)-(III) and the relation  $[\text{H}^+] = [\text{D}^+] = [e]/2$ , the rate equations for  $[\text{H}]$  and  $[\text{D}]$  can be written in the form (we again omit the vibrational level subscript for brevity)

$$\begin{aligned} \frac{d[\text{H}]}{dt} = & (K_1 + \frac{1}{2}K_{14})[e][\text{H}_2] + (K_{13b} + \frac{1}{2}K_{24})[e][\text{HD}] + K_{11}[e][\text{H}^-] \\ & + K_{27}[e][\text{H}_2^+] + K_{29b}[e][\text{HD}^+] + \frac{1}{2}K_{18}[e][\text{D}_2] - K_{38}[e][\text{H}] \end{aligned} \quad (27)$$

$$\begin{aligned} \frac{d[\text{D}]}{dt} = & (K_3 + \frac{1}{2}K_{16})[e][\text{D}_2] + (K_{13a} + \frac{1}{2}K_{24})[e][\text{HD}] + K_{11}[e][\text{D}^-] \\ & + K_{28}[e][\text{D}_2^+] + K_{29a}[e][\text{HD}^+] + \frac{1}{2}K_{19}[e][\text{H}_2] - K_{39}[e][\text{D}] \end{aligned} \quad (28)$$

The rate equations for  $[\text{H}^-]$ ,  $[\text{D}^-]$ ,  $[\text{H}_2^+]$ ,  $[\text{D}_2^+]$  and  $[\text{HD}^+]$  are given by Eqs. (15)–(19), and their solutions are given by Eq. (21). The terms in Eqs. (27) and (28) containing  $K_{18}$  and  $K_{19}$  originate from the CX-MAD mechanism. They make the production of one atomic isotope to depend on the molecular concentration of the other isotope.

We now recall that the characteristic timescale for the evolution of  $[\text{H}^-]$  and  $[\text{D}^-]$  is  $\tau_{\text{H}^-}$ , and that for the evolution of  $[\text{H}_2^+]$ ,  $[\text{D}_2^+]$  and  $[\text{HD}^+]$  is  $\tau_{\text{H}_2^+}$ . For the evolution of  $[\text{H}]$  and  $[\text{D}]$ , there is also another characteristic timescale, ( $K_{38} = K_{39}$ ),  $\tau_{ion} = 1/K_{38}[e]$  on which the ground state atoms  $\text{H}$  and  $\text{D}$  are ionized by electron impact. For  $[e] = 10^{14} \text{ cm}^{-3}$  and  $T=1, 2$  and  $3 \text{ eV}$ , the values of  $\tau_{ion}$  are (we take  $K_{38}$  from the collisional-radiative model for  $\text{H}$ ):  $0.19\text{s}$ ,  $0.34 \times 10^{-3}\text{s}$  and  $0.28 \times 10^{-4}\text{s}$ . The values of  $\tau_{\text{H}^-}$  and  $\tau_{\text{H}_2^+}$  given in the preceding subsection are three to six orders of magnitude smaller than  $\tau_{ion}$  indicating that on the timescale of  $\tau_{ion}$  the equilibrium values for  $[\text{H}^-]$ ,

### 2.3 Rate equations for MAD kinetics

---

$[D^-]$ ,  $[H_2^+]$ ,  $[D_2^+]$  and  $[HD]$  have already been reached. Introducing the steady-state concentrations for these species into Eqs. (27) and (28), we find the solutions for  $[\underline{H}]$  and  $[\underline{D}]$  in the form

$$[\underline{H}] = \frac{1}{2K_{38}} \left\{ (1 + \eta_1)(2K_1[H_2] + K_{13}[HD]) + (1 + \eta_2)K_{24}[HD] + [(1 + \eta_3)K_{14} + \eta_3K_{19}][H_2] + K_{18}[D_2] \right\} (1 - e^{-t/\tau_{ion}}) \quad (29)$$

$$[\underline{D}] = \frac{1}{2K_{38}} \left\{ (1 + \eta_1)(2K_3[D_2] + K_{13}[HD]) + (1 + \eta_2)K_{24}[HD] + [(1 + \eta_3)K_{16} + \eta_3K_{18}][D_2] + K_{19}[H_2] \right\} (1 - e^{-t/\tau_{ion}}) \quad (30)$$

where

$$\eta_1 = \frac{K_{11}}{K_2 + K_{11}}, \quad \eta_2 = \frac{K_{29}}{K_{26} + K_{29}}, \quad \eta_3 = \frac{K_{27}}{K_{15} + K_{27}}. \quad (31)$$

From Eqs. (29), (30) we obtain for the ratio  $R_{H/D}^{MAD} = [\underline{H}]/[\underline{D}]$  (for a given vibrational level  $v$ )

$$\begin{aligned} R_{H/D,v}^{MAD} &= \left( (1 + \eta_1)(2K_{1,v}[H_2]_v + K_{13,v}[HD]_v) + (1 + \eta_2)K_{24,v}[HD]_v \right. \\ &\quad \left. + [(1 + \eta_3)K_{14,v} + \eta_3K_{19,v}][H_2]_v + K_{18,v}[D_2]_v \right) \\ &\quad / \left( (1 + \eta_1)(2K_{3,v}[D_2]_v + K_{13,v}[HD]_v) + (1 + \eta_2)K_{24,v}[HD]_v \right. \\ &\quad \left. + [(1 + \eta_3)K_{16,v} + \eta_3K_{18,v}][D_2]_v + K_{19,v}[H_2]_v \right) \end{aligned} \quad (32)$$

We note that the branching ratios  $\eta_i$ , Eqs. (31) are related to  $\chi_i$ , Eqs. (24) by  $\chi_i + \eta_i = 1$ . By virtue of earlier mentioned fact that electron impact dissociative recombination and dissociative excitation processes of molecular ions do not show isotope effects [26] (i.e.  $K_{15} = K_{17} = K_{26}$  and  $K_{27} = K_{28} = K_{29}$ ), one has  $\chi_2 = \chi_3$  and  $\eta_2 = \eta_3$ .

The solution (29) and (30) for  $[\underline{H}]$  and  $[\underline{D}]$  are valid as long as the basic assumption of our treatment of the rate equation,  $[\underline{H}], [\underline{D}] \ll [H_2], [D_2], [HD], [e]$ , is not violated. This condition limits the validity of these solutions to times of the order of magnitude of  $\tau_{H^-}$  and  $\tau_{H_2^+}$  equilibrium times (or a few times larger). This restriction on the validity of Eqs. (29) and (30) does not, however, affects the validity of the ratio  $R_{H/D,v}^{MAD}$ .

### 3 Total isotope enhancement factors, $R_{\text{H/D}}^{\text{MAR}}$ and $R_{\text{H/D}}^{\text{MAD}}$

The magnitude of isotope effects in MAR and MAD can be obtained only after summing  $[\text{H}^*]_v$ ,  $[\text{D}^*]_v$  and  $[\text{H}]_v$ ,  $[\text{D}]_v$  over vibrational population distributions in  $\text{H}_2$ ,  $\text{D}_2$  and  $\text{HD}$ . Assuming that the vibrational population distribution function  $f(v)$  is the same for all three isotopomers. We now introduce the notation

$$S_{j,\text{AB}}^\lambda = \sum_v K_{j,\text{AB}(v)}^\lambda f(v), \quad [\text{AB}]_v = f(v)[\text{AB}], \quad \sum_v [\text{AB}]_v = [\text{AB}], \quad (33)$$

where  $\text{AB}$  is either of  $\text{H}_2$ ,  $\text{D}_2$  or  $\text{HD}$ ,  $j$  is the reaction number from Table 1,  $[\text{AB}]$  is the total number of  $\text{AB}$  molecules, and  $\lambda$  is the label of reaction type, for example: e.g.  $\text{da}$ =dissociative attachment,  $\text{ic}$ =ion conservation,  $\text{cx}$ =charge exchange (electron capture),  $\text{px}$ =particle exchange ( $\text{ic}=\text{cx}+\text{pc}$ ). One then obtains for isotope enrichment factors for MAR and MAD processes, respectively,

$$R_{\text{H/D}}^{\text{MAR}} = \frac{\sum_v [\text{H}^*]_v}{\sum_v [\text{D}^*]_v}, \quad R_{\text{H/D}}^{\text{MAD}} = \frac{\sum_v [\text{H}]_v}{\sum_v [\text{D}]_v} \quad (34)$$

the expressions

$$\begin{aligned} R_{\text{H/D}}^{\text{MAR}} &= \left[ \omega_\chi \{ S_{1,\text{H}_2}^{\text{da}} [\text{H}_2] + S_{3,\text{D}_2}^{\text{da}} [\text{D}_2] + S_{13,\text{HD}}^{\text{da}} [\text{HD}] \} + S_{24,\text{HD}}^{\text{cx}} [\text{HD}] \right. \\ &\quad \left. + (S_{14,\text{H}_2}^{\text{ic}} + S_{19,\text{H}_2}^{\text{cx}}) [\text{H}_2] \right] \\ &\quad / \left[ \omega_\chi \{ S_{1,\text{H}_2}^{\text{da}} [\text{H}_2] + S_{3,\text{D}_2}^{\text{da}} [\text{D}_2] + S_{13,\text{HD}}^{\text{da}} [\text{HD}] \} + S_{24,\text{HD}}^{\text{cx}} [\text{HD}] \right. \\ &\quad \left. + (S_{16,\text{D}_2}^{\text{ic}} + S_{18,\text{D}_2}^{\text{cx}}) [\text{D}_2] \right] \end{aligned} \quad (35)$$

$$\begin{aligned} R_{\text{H/D}}^{\text{MAD}} &= \left[ \omega_\eta \{ 2S_{1,\text{H}_2}^{\text{da}} [\text{H}_2] + S_{13,\text{HD}}^{\text{da}} [\text{HD}] \} + S_{24,\text{HD}}^{\text{cx}} [\text{HD}] \right. \\ &\quad \left. + (S_{14,\text{H}_2}^{\text{ic}} + \xi S_{19,\text{H}_2}^{\text{cx}}) [\text{H}_2] + \zeta S_{18,\text{D}_2}^{\text{cx}} [\text{D}_2] \right] \\ &\quad / \left[ \omega_\eta \{ 2S_{3,\text{D}_2}^{\text{da}} [\text{D}_2] + S_{13,\text{HD}}^{\text{da}} [\text{HD}] \} + S_{24,\text{HD}}^{\text{cx}} [\text{HD}] \right. \\ &\quad \left. + (S_{16,\text{D}_2}^{\text{ic}} + \xi S_{18,\text{H}_2}^{\text{cx}}) [\text{D}_2] + \zeta S_{19,\text{H}_2}^{\text{cx}} [\text{H}_2] \right] \end{aligned} \quad (36)$$

where

$$\omega_\chi = \frac{\chi_1}{\chi_2}, \quad \omega_\eta = \frac{1 + \eta_1}{1 + \eta_2}, \quad \xi = \frac{\eta_2}{1 + \eta_2}, \quad \zeta = \frac{1}{1 + \eta_2} \quad (37)$$

### 3 Total isotope enhancement factors

---

The terms in curly brackets in expressions (35) and (36) for  $R_{\text{H/D}}^{\text{MAR}}$  and  $R_{\text{H/D}}^{\text{MAD}}$  originate from the NI channels of MAR and MAD, while the remaining terms in these expressions originate from the IC and CX-MAD channels. It is important to note that the NI terms in the nominator and denominator in  $R_{\text{H/D}}^{\text{MAR}}$  are identical, which is a consequence of earlier mentioned isotopic symmetry of reaction kinetics of this MAR channel. The corresponding NI terms in nominator and denominator of  $R_{\text{H/D}}^{\text{MAD}}$  are, however, different and can generate an isotope effect in MAD. We see also from Eqs. (35), (36) that both NI and IC terms of MAR and MAD, related to [HD], appear symmetrically in the nominators and denominators of  $R_{\text{H/D}}^{\text{MAR}}$  and  $R_{\text{H/D}}^{\text{MAD}}$  and, therefore, reactions involving HD molecules do not produce any isotopic effect in MAR nor MAD. The IC terms in the nominators and denominators of  $R_{\text{H/D}}^{\text{MAR}}$  and  $R_{\text{H/D}}^{\text{MAD}}$  are different and this difference is the main source of the isotopic effect in MAR. The presence of other terms in  $R_{\text{H/D}}^{\text{MAR}}$  only dilutes the ratio of IC terms associated with  $[\text{H}_2]$  and  $[\text{D}_2]$  in Eq. (35).

The isotope effect in MAD is expected to be more pronounced than in MAR because of the non-zero contribution of NI MAD channel to  $R_{\text{H/D}}^{\text{MAD}}$ . In fact, as will be seen later on, this is the dominant channel producing the isotope effect in MAD.

The values of quantities  $S_{j,\text{AB}}^\lambda$ ,  $\omega_\chi$ ,  $\omega_\eta$ ,  $\xi$  and  $\zeta$  needed to calculate  $R_{\text{H/D}}^{\text{MAR}}$  and  $R_{\text{H/D}}^{\text{MAD}}$  are given in Table 2 for  $T = 1, 2$  and  $3$  eV. A Boltzmann distribution was assumed for the vibrational level populations in the molecules. The references from which the corresponding rate coefficients  $K_{j,\text{AB}(v)}^\lambda(T)$  were taken are also given in this table. In Ref. [13] detailed calculations were made only for  $K_{14,\text{H}_2(v)}^{\text{ic}}(T)$ . For a given value of  $T$ , the function  $K_{14,\text{H}_2(v)}^{\text{ic}}(v) = F(E_{\text{vib}}(v))$ , where  $E_{\text{vib}}(v)$  is the vibrational energy of  $\text{H}_2(v)$ , shows a smooth behavior, except for the jump at  $E_{\text{vib}}(v = 4)$ , when reaction 14 becomes exothermic (for  $v \geq 4$ ).  $F(E_{\text{vib}}(v))$  sharply increases with increasing  $v$ , and then slowly decreases with the further increase of  $v$ . Because of the dominance of CX channel in the IC process, and identity of electronic structure of three-atomic hydrogen isotope molecular ions, the function  $F(E_{\text{vib}}(V))$  is the same also for the IC reactions in the  $\text{D}^+ + \text{D}_2$  and the  $\text{H}^+ / \text{D}^+ + \text{HD}$  collision systems. This has been shown also by the limited number of  $\text{D}^+ + \text{D}_2$  and  $\text{T}^+ + \text{T}_2$  cross sectional calculations in Ref.



### 3 Total isotope enhancement factors

---

[13]. Therefore, using the identity of  $F(E_{vib}(v))$  for three-atomic hydrogen isotope molecular ion systems, one can determine the values of  $K_{16,D_2}^{ic}(v)$  and  $K_{HD}^{ic}(v)$ . The data for  $K_{19,H_2}^{cx}(T)$  are also known from Ref. [13].

The values of  $S_{18,D_2}^{cx}(T)$  and  $S_{24,HD}^{cx}(T)$  can be determined by assuming that the ratios  $S_{18,D_2}^{cx}/S_{16,D_2}^{ic}$  and  $S_{24,HD}^{cx}/S_{HD}^{ic}$  are the same as  $S_{19,H_2}^{cx}/S_{14H_2}^{ic}$  for a given temperature  $T$ .

It should be noted that the dominant contribution to  $S_{j,AB}^\lambda$  comes from the high- $v$  terms,  $s_{j,AB}^\lambda(v) = f(v)K_{j,AB}^\lambda$  in the sum (33). The fact that in DA reactions the isotope effect rapidly decreases with increasing  $v$ , leads to a relatively small ratio  $S_{1,H_2}^{da}/S_{1,D_2}^{da} \simeq 1.41$ , compared with the value  $s_{1,H_2}^{da}(v=0)/s_{3,D_2}^{da}(v=0) \sim 400$  for  $T=1$  eV. It can be rigorously shown that the original  $\exp(-\mu^{1/2})$  mass dependence of  $K_{AB}^{da}(v)$  [20], where  $\mu$  is the reduced mass of A and B, after averaging over the Boltzmann distribution of vibrational level populations leads to  $S_{AB}^{da} \sim \mu^{-1/2}$ , as can be verified by the ratios of  $S_{j,AB}^{da}$  values given in Table 2.

The isotope effect in the IC MAR and MAD channels is also obvious from the  $S_{j,AB}^{ic}$  values in Table 2; It is, however, much smaller:  $S_{14,H_2}^{ic}/S_{16,D_2}^{ic} \simeq 1.05$ , for  $T=1$  eV.

From the expressions (35) and (36) for  $R_{H/D}^{MAR}$  and  $R_{H/D}^{MAD}$ , it is evident that these ratios also depend on the mutual ratios of  $[H_2]$ ,  $[D_2]$  and  $[HD]$ . One can consider  $R_{H/D}^{MAR}$  and  $R_{H/D}^{MAD}$ , as defined by Eqs. (35) and (36), as measures of isotope effects in MAR and MAD kinetics only if  $[H_2]=[D_2]$ . In this case, the values of  $R_{H/D}^{MAR}$  and  $R_{H/D}^{MAD}$ , with the values of  $S_{j,AB}^\lambda$  from Table 2, are always greater than one (and tend to one only when  $[HD] \gg [H_2], [D_2]$ ), indicating that kinetics of both MAR and MAD mechanisms exhibit an isotope effect. The  $H^+$  ions recombine with plasma electrons faster than the  $D^+$  ions, while  $H_2$  molecules dissociate faster than  $D_2$ . The isotope effect, inherent in DA and IC reactions, is therefore, not eliminated in the overall plasma recombination and molecule dissociation kinetics after averaging over the vibrational level populations.  $R_{H/D}^{MAR}$  and  $R_{H/D}^{MAD}$  have maximum values for  $[HD]=0$ .

In Table 3 we give the values of  $R_{H/D}^{MAR}$  and  $R_{H/D}^{MAD}$  for  $T = 1, 2$  and  $3$  eV and several values of the ratio  $[H_2]:[D_2]:[HD]$ . The smearing out effect of the increase of  $[HD]$  on  $R_{H/D}^{MAR}$  and  $R_{H/D}^{MAD}$  is obvious. For a given temper-

### 3 Total isotope enhancement factors

---

ature,  $R_{\text{H/D}}^{MAD}$  is always considerably larger than  $R_{\text{H/D}}^{MAR}$ , but this difference decreases with the increase of [HD]. For a given ratio  $[\text{H}_2]:[\text{D}_2]:[\text{HD}]$ ,  $R_{\text{H/D}}^{MAD}$  slowly decreases when plasma temperatures increases, while  $R_{\text{H/D}}^{MAR}$  shows a mild maximum at  $T = 2$  eV. The origin of this maximum in  $R_{\text{H/D}}^{MAR}$  is the maximum of  $S_{j,AB}^{da}(T)$  at this temperature (see Table 2), while the decrease of  $R_{\text{H/D}}^{MAD}$  with increasing  $T$  is a result of the rapid increase with  $T$  of IC terms in Eq. (36) (that reduces the dominating role of NI terms in determining the  $R_{\text{H/D}}^{MAD}$  value).

In conclusion, the isotope effects in MAR and MAD in the temperature range 1-3 eV (with the general assumption  $[e] \leq 5 \times 10^{14} \text{ cm}^{-3}$ ) and concentration ratios  $[\text{H}_2]:[\text{D}_2]:[\text{HD}]$  in the range 1:1:0 - 1:1:2, are 2%-4% for MAR and 5%-14% for MAD.

A note should be made regarding the applicability of Eqs. (35), (36) to the case  $[\text{HD}]=0$ . In deriving Eqs. (35), (36) we have considered HD as a “reservoir” particle and for that reason have neglected HD production and destruction reactions 20, 22, and 30, 32, respectively, in MAR and MAD kinetics. If HD is not a “reservoir” particle, these reaction must be included in the kinetics. Accurate expressions for  $R_{\text{H/D}}^{MAR}$  and  $R_{\text{H/D}}^{MAD}$  derived for this case, and subsequent estimates of their numerical values for  $T=1, 2$  and 3 eV, show that the values for  $R_{\text{H/D}}^{MAR}$  and  $R_{\text{H/D}}^{MAD}$  shown in Table 3 for  $[\text{HD}]=0$  should be reduced by 0.3-0.4% (e.g. the value 1.032 for  $T=1$  eV becomes 1.028). In realistic H/D divertor plasmas, however, the amount of HD molecules is expected to be substantial.

The knowledge of total rate coefficients  $S_{j,AB}^{\lambda}$  for the reactions involved in MAR and MAD kinetics (see Table 2) allows one to calculate  $[\text{H}^*]$  and  $[\text{H}]$  from Eqs. (25) and (29), respectively, by averaging them over the distribution function  $f(v)$  of vibrational level populations. For the characteristic time  $t_0 = \max\{\tau_{\text{H}^-}, \tau_{\text{H}_2^+}\}$  over which MAR kinetics equilibrium is achieved, the values for  $[\text{H}^*]$  for  $T=1, 2$  and 3 eV, neutral composition  $[\text{H}_2]:[\text{D}_2]:[\text{HD}]=1:1:1$  and electron density  $[e] = 10^{14} \text{ cm}^{-3}$  are  $3.9 \times 10^{-2} [\text{H}_2]$ ,  $2.4 \times 10^{-2} [\text{H}_2]$  and  $0.87 \times 10^{-2} [\text{H}_2]$ , respectively. These values include also the branching factors  $A_3/(K_7[e] + A_3)$  for stabilization of  $[\text{H}^*]$  to the ground state.

During the same time  $\tau_0$ , and for the same plasma conditions, the con-

#### 4 Cumulative MAR and MAD isotope effects

---

centration of  $[\underline{\text{H}}]$  attains the values  $4.1 \times 10^{-2} [\text{H}_2]$ ,  $9.0 \times 10^{-2} [\text{H}_2]$  and  $9.8 \times 10^{-2} [\text{H}_2]$  for  $T=1, 2$  and  $3$  eV, respectively. The obtained numbers indicate that over timescales characteristic for MAR and MAD processes, our treatment of rate equations does not violate the condition  $[\text{H}^*], [\underline{\text{H}}] \ll [\text{H}_2]$ . The above numbers also indicate that while for  $T = 1$  eV,  $[\text{H}^*]$  is about the same as  $[\underline{\text{H}}]$ , for  $T = 2$  and  $3$  eV  $[\underline{\text{H}}]$  becomes about four and ten times larger than  $[\text{H}^*]$ , respectively.

#### 4 Cumulative MAR and MAD isotope effects - during the ion residence time in divertor region

The values of  $R_{\text{H/D}}^{\text{MAR}}$  and  $R_{\text{H/D}}^{\text{MAD}}$  obtained in the preceding section are pertinent to one cycle of operation of MAR and MAD mechanisms, respectively. The ground state H(1s) or D(1s) atoms, created by these mechanisms, can be ionized by plasma electrons, and produce ions which enter new MAR and MAD cycles. A cumulative effect of these mechanisms is possible only if the ion residence time in the divertor,  $\tau_{\text{res}}$ , is larger than the (re-) ionization time  $\tau_{\text{ion}}$  of ground state hydrogen atom. To simplify the problem of determining  $\tau_{\text{res}}$ , we shall assume that the ion velocity in divertor channel is equal to ionic sound speed, which, for a given (divertor magnetic field line) connection length  $L$  between entrance and target, would give an estimate for the lowest value of the divertor ion residence time  $\tau_{\text{res}}$ . For plasma temperatures ( $T_e = T_i$ ) of 1, 2 and 3 eV and a typical divertor connection length  $L = 10$  m, the ion residence times then are: 0.72 ms, 0.51 ms and 0.42 ms, respectively. By taking the electron-impact ionization rates for H(1s) from the collisional-radiative model for  $T = 1, 2$  and  $3$  eV and  $[e] = 10^{14} \text{ cm}^{-3}$ , one obtains (re-) ionization times for H of 190 ms, 0.775 ms and 0.0282 ms, respectively. For a plasma density of  $[e] = 3 \times 10^{14} \text{ cm}^{-3}$ , the corresponding ionization times are 32 ms, 0.155 ms and 0.0065 ms, respectively. The ratio

$$n_0 = \frac{\tau_{\text{res}}}{\tau_{\text{ion}}} \quad (38)$$

defines the number of MAR and MAD cycles that a hydrogenic plasma ion flowing into the divertor can make during its residence time in the divertor

## 5 Isotope Ion Charge Separation

---

region. The cumulative isotope effect of MAR and MAD mechanisms is then expressed as

$$r_0^M = (R_{H/D}^M)^{n_0}, \quad M = MAR \text{ or } MAD. \quad (39)$$

$r_0^{MAD}$  is a measure of the relative H atom enrichment over D during the residence time of its ion in the divertor, and  $r_0^{MAR}$  is a measure of  $H^+$  and  $D^+$  charge separation during that time. For  $T = 1$  eV,  $\tau_{res} \ll \tau_{ion}$  for both plasma densities,  $[e] = 1 \times 10^{14} \text{ cm}^{-3}$  and  $[e] = 3 \times 10^{14} \text{ cm}^{-3}$ . For  $T = 2$  eV, however,  $\tau_{res}/\tau_{ion}$  is 0.66 and 3.29 for these two densities, respectively, and for  $T = 3$  eV the corresponding values are 14.9 and 64.6.

With these values of  $\tau_{res}/\tau_{ion}$ , we have calculated  $r_0^{MAR}$  and  $r_0^{MAD}$  for  $T = 2$  eV and 3 eV and several  $[H_2]:[D_2]:[HD]$  ratios. The results for  $r_0^{MAR}$  are given in Table 4, and those for  $r_0^{MAD}$  are shown in Table 5. As obvious from Eq. (39), the values of  $r_0^M$  are highly sensitive to the value of  $n_0$ . For  $[H_2]:[D_2]:[HD]=1:1:1$ , for instance,  $r_0^{MAR}$  for  $T = 2$  eV and  $[e] = 10^{14} \text{ cm}^{-3}$  is only 1.018, while for  $T = 3$  eV and  $[e] = 3 \times 10^{14} \text{ cm}^{-3}$  it is 4.34. The corresponding values for  $r_0^{MAD}$  are 1.06 and 162.1. The values of  $r_0^{MAR}$  and  $r_0^{MAD}$  in Table 4 and 5 show that the cumulative MAR and MAD effects can be significant when  $n_0$  is considerably larger than one.  $n_0$  contains a linear dependence on  $L$ , a stronger than linear dependence on  $[e]$ , and increases very sharply with increasing  $T$  in the region  $T \lesssim 5$  eV. As the numbers in Tables 4 and 5 show, relatively small changes in  $[e]$  and  $T$  produce dramatic changes in the values of  $r_0^{MAR}$  and  $r_0^{MAD}$ .

Similar strong effects on  $r_0^M$  are produced also by the variation of  $L$ . For  $L = 15$  m, the value of  $n_0$  for  $T = 3$  eV and  $[e] = 3 \times 10^{14} \text{ cm}^{-3}$  becomes 96.6 which leads to an increase of  $r_0^{MAR}$  and  $r_0^{MAD}$  by about a factor of two and ten, respectively, for the ratios  $[H_2]:[D_2]:[HD]$  given in Tables 4 and 5.

## 5 Isotope Ion Charge Separation

We have mentioned in the Introduction that the MAR isotope effect acts as an isotope ion charge separation mechanism: while enhancing the recombination of  $H^+$  ions with plasma electrons it, at the same time, enriches the relative content of  $D^+$  in the plasma. We have also mentioned two

## 5.1 CX-MAD isotope ion conversion

---

additional isotope ion charge separation mechanisms operative in the H/D divertor plasma: the CX-MAD, as exemplified by reaction chains (9) and (10) for instance, and the direct isotope ion conversion (e.g. reaction chains (11)). Since larger abundances of one of the isotopic ions over the others would have significant consequences on plasma transport, the fuel cycle in a reactor, and possibly other properties, in the present section we shall estimate the contributions of CX-MAD and direct isotope ion conversion (DIIC) reactions as ion charge separation mechanisms.

### 5.1 CX-MAD isotope ion conversion

As can be easily verified, the pairs of processes 18, 28 and 21, 29b of Table 1 each form a CX-MAD reaction chain and lead to a  $H^+ \rightarrow D^+$  ion conversion. The pairs of processes 19, 27 and 23, 29a of Table 1 also form CX-MAD reaction chains, but lead to  $D^+ \rightarrow H^+$  ion conversion.

Since the rate coefficients of particle exchange reactions 21 and 23 are much smaller than those of charge exchange reactions 18 and 19, respectively, we shall neglect the contributions of 21, 29b and 23, 29a CX-MAD reaction chains to the overall CX-MAD ion isotope conversion mechanism.

Using reactions 18, 28, 38 and 39, we see that one  $H^+ \rightarrow D^+$  isotope exchange is accompanied by appearance of one  $\underline{H}$  atom via reaction 18 and of one  $\underline{D}$  atom via reaction 28. Hence one can write the rate equation for  $H^+ \rightarrow D^+$  ion conversion in the form

$$\frac{d([\underline{H}_{18}] + [\underline{D}_{28}])}{dt} = K_{18}[H^+][D_2] + K_{28}[e][D_2^+] - K_{38}[e]([\underline{H}_{18}] + [\underline{D}_{28}]) \quad (40)$$

where the equality  $K_{38} = K_{39}$  has been used.

In a similar way, from reaction 19, 27, 38 and 39, one obtains the rate equation for  $D^+ \rightarrow H^+$  ion conversion

$$\frac{d([\underline{D}_{19}] + [\underline{H}_{27}])}{dt} = K_{19}[D^+][H_2] + K_{27}[e][H_2^+] - K_{38}[e]([\underline{D}_{18}] + [\underline{H}_{27}])$$

$[H_2^+]$  and  $[D_2^+]$  in these equations satisfy Eqs. (17) and (18), respectively, the solutions of which have the form given by Eq. (21). Using the fact that in the temperature range of interest here,  $\tau_{ion}$  is several orders of magnitude

## 5.1 CX-MAD isotope ion conversion

---

larger than  $\tau_{H_2^+}$  and  $\tau_{D_2^+}$  ( $\simeq \tau_{H_2^+}$ ) as discussed in Section 2, the solutions of Eqs. (40) and (41) can be written in the form (when  $[H_2^+]$  and  $[D_2^+]$  are replaced by their equilibrium values  $[H_2^+]_\infty$  and  $[D_2^+]_\infty$ ):

$$([H] + [D])^{CX-MAD} = \frac{1}{2K_{38}} \left\{ [(1 + \eta'_3)K_{18} + \eta'_3 K_{16}] [D_2] \right\} (1 - e^{-t/\tau_{ion}}) \quad (42)$$

$$([D] + [H])^{CX-MAD} = \frac{1}{2K_{38}} \left\{ [(1 + \eta_3)K_{19} + \eta_3 K_{14}] [H_2] \right\} (1 - e^{-t/\tau_{ion}}) \quad (43)$$

where  $\eta_3$  has been defined earlier, Eq. (31), and  $\eta'_3 = K_{28}/(K_{17} + K_{28}) \simeq \eta_3$  (in view of the relations  $K_{15} \simeq K_{17}$  and  $K_{27} \simeq K_{28}$ ). Equations (40)–(43) are valid for each vibrational level of excited  $H_2(v)$  and  $D_2(v)$  molecules. After averaging over the populations of  $H_2(v)$  and  $D_2(v)$ , we obtain for the ratio

$$R_{H^+/D^+}^{CX-MAD} = \frac{\sum_v ([D]_v + [H]_v)}{\sum_v ([H]_v + [D]_v)} \quad (44)$$

the expression (compare to Eqs. (35) and (36))

$$R_{H^+/D^+}^{CX-MAD} = \frac{r(D^+ \rightarrow H^+)}{r(H^+ \rightarrow D^+)} = \frac{\{S_{19,H_2}^{cx} + \eta_3(S_{14,H_2}^{ic} + S_{19,H_2}^{ic})\} [H_2]}{\{S_{18,D_2}^{cx} + \eta_3(S_{16,D_2}^{ic} + S_{18,D_2}^{ic})\} [D_2]} \quad (45)$$

We have introduced the notation  $r(A^+ \rightarrow B^+)$  to indicate the direction of isotope ion conversion. The ratio  $R_{H^+/D^+}^{CX-MAD}$  does not depend on  $[HD]$ ; a consequence of the (justified) neglect of the contributions of CX-MAD reaction chains 21, 29b and 23, 29a to  $([H] + [D])^{CX-MAD}$  and  $([D] + [H])^{CX-MAD}$ , respectively.

With the values of  $S_{j,AB}^\lambda$  from Table 2, and with the values for  $\eta_3$  of 0.233, 0.589 and 0.710 for  $T=1, 2$  and  $3$  eV [11],[26], we obtain for the ratio  $R_{H^+/D^+}^{CX-MAD}$  the values 1.055, 1.054 and 1.036 for these three temperatures (and for  $[H_2]:[D_2] = 1$ ). It appears that the CX-MAD mechanism favors the conversion  $D^+ \rightarrow H^+$  over  $H^+ \rightarrow D^+$ . The effect on isotope ion

## 5.2 Direct isotope ion conversion reactions (DIIC)

---

charge separation is opposite to that of MAR. The cumulative effect of CX-MAD on the isotope ion conversion during an ion divertor residence time,  $\left(R_{\text{H}^+/\text{D}^+}^{\text{CX-MAD}}\right)^{n_0}$ , for  $T=2$  and  $3$  eV is 1.035 and 1.69 for  $[e] = 10^{14} \text{ cm}^{-3}$  and 1.19 and 9.82, for  $[e] = 3 \times 10^{14} \text{ cm}^{-3}$ , respectively. Comparing these values with those for  $\left(R_{\text{H}^+/\text{D}^+}^{\text{MAR}}\right)^{n_0}$  in Table 4, one concludes that CX-MAD, which favors the  $\text{D}^+ \rightarrow \text{H}^+$  ion conversion, is a stronger ion charge separation mechanism than MAR.

## 5.2 Direct isotope ion conversion reactions (DIIC)

The particle exchange reaction 20 and 30 in Table 1 directly convert  $\text{H}^+$  ions into  $\text{D}^+$  ions, while reactions 22 and 32 do the opposite. The ratio of the rates of  $\text{D}^+ \rightarrow \text{H}^+$  and  $\text{H}^+ \rightarrow \text{D}^+$  conversion (px denotes “particle exchange”)

$$R_{\text{H}^+/\text{D}^+}^{\text{dir}} = \frac{r(\text{D}^+ \rightarrow \text{H}^+)}{r(\text{H}^+ \rightarrow \text{D}^+)} = \frac{S_{22,\text{H}_2}^{\text{px}}[\text{H}_2] + S_{32,\text{HD}}^{\text{px}}[\text{HD}]}{S_{20,\text{D}_2}^{\text{px}}[\text{D}_2] + S_{30,\text{HD}}^{\text{px}}[\text{HD}]} \quad (46)$$

where  $S_{j,\text{AB}}^{\text{px}}$  are  $v$ -population averaged rate coefficients of molecule  $\text{AB}(v)$ . We note that the pairs of reactions 20, 32 and 22, 30 are inverse to each other. For the ground vibrational states of  $\text{H}_2$ ,  $\text{HD}$  and  $\text{D}_2$ , reactions 22 and 32 are slightly exothermic (by 0.0394 eV and 0.0462 eV, respectively) while reactions 20 and 30 are endothermic. On the basis of the detailed balance principle, relating the rate coefficients of mutually inverse reactions, the ratio  $R_{\text{H}^+/\text{D}^+}^{\text{dir}}$  for  $v = 0$  states of  $\text{H}_2$ ,  $\text{HD}$  and  $\text{D}_2$  should be larger than one (i.e.:  $\text{D}^+ \rightarrow \text{H}^+$  conversion should be more efficient than  $\text{H}^+ \rightarrow \text{D}^+$ ). In view of the larger number of states in the heavier molecule, and after averaging over the vibrational populations, the situation may be changed to the opposite. No detailed,  $v$ -resolved cross section calculations are presently available for all the above direct ion conversion processes.

The recent  $v$ -resolved cross section calculation for reaction 20 of Table 1 [28] indicate that the  $v$ -dependence of  $\sigma_{20}^{\text{px}}$  is relatively weak (but still up to a factor two). For energies below  $\sim 5$  eV,  $\sigma_{20}^{\text{px}}(v)$  decreases with increasing  $v$ , while for  $E \gtrsim 6$  eV the opposite is true. The direct experimental measurements of rate coefficient  $K_{20}^{\text{px}}$  (the data being collected in Ref. [24]) differ by

## 6 Concluding Remarks

---

a factor 2 to 3 in the temperature range 0.5–2 eV. The large dispersion of experimental  $K_{20}^{px}$  data may result, besides from uncertainties in the applied measurement methods, also from different vibrational populations of  $D_2(v)$  in these experiments. The experimental situation for  $K_{22}^{px}$  is similar.

In absence of reliable information on the rate coefficients  $K_{j,AB}^{px}(v)$  for the ion conversion reactions 20, 22, 30 and 32, it is impossible at present to estimate the accurate values for  $R_{H^+/D^+}^{dir}$  in the temperature range 1–3 eV. The “preferred” data for  $K_{20}^{px}$ ,  $K_{22}^{px}$ ,  $K_{30}^{px}$  and  $K_{32}^{px}$  derived by taking an average of experimental data (for  $K_{20}^{px}$  and  $K_{22}^{px}$ ), or by using the detailed balance principle (for  $K_{30}^{px}$  and  $K_{32}^{px}$ , assuming ground state reactants and products), cannot be considered as adequate to calculate  $R_{H^+/D^+}^{dir}$  (even for the case of  $v = 0$  states).

Without an accurate estimate of  $R_{H^+/D^+}^{dir}$ , the question on isotope ion charge exchange separation in a divertor plasma remains at present unanswered.

## 6 Concluding Remarks

In the present paper we have investigated the isotope effect in molecule assisted plasma recombination (MAR) and molecular gas dissociation (MAD) in a H/D plasma in the temperature range  $0.5 \text{ eV} \lesssim T \lesssim 4.5 \text{ eV}$  and for plasma densities below  $\sim 5 \times 10^{14} \text{ cm}^{-3}$ . The analysis of relevant rate equations for the products of MAR and MAD reactions chains shows that the isotope effect is present both in MAR and MAD even after averaging over the distribution of vibrational populations of molecules. For  $T = 1 - 3 \text{ eV}$  and  $[e] = (1 - 3) \times 10^{14} \text{ cm}^{-3}$ , the MAR and MAD isotope effects are in the range 1%-4% and 2%-14%, respectively, depending on the values of  $[H_2]:[D_2]:[HD]$  ratio. During the ion residence time in divertor the differences in the isotopic products of MAR and MAD processes may be quite large for  $T \gtrsim 1.5 \text{ eV}$ .

The analysis of the problem was done under the assumption that the amount of the products  $H^*$  of MAR and  $\underline{H}$  of MAD processes in the plasma are still considerably smaller than the concentrations of major divertor plasma constituents  $[e]$ ,  $[H^+]$ ,  $[D^+]$ ,  $[H]$ ,  $[D]$ ,  $[H_2]$ ,  $[D_2]$  and  $[HD]$ . This re-



## 6 Concluding Remarks

---

striction in the treatment of the problem was introduced to obtain an analytically tractable system of rate equations, and because the primary purpose of the present work was to investigate whether MAR and MAD mechanisms in principle generate different amounts of their isotopic products (after averaging over the populations of their internal states). This limitation can easily be removed if one would opt to solve the rate equations for all plasma constituents numerically.

The list of reactions given in Table 1 should then be expanded also by reactions of direct electron impact dissociation of molecules and by the reactions of the type given by Eqs. (7), (8) and (12) for all isotopic species. Such complete treatment of the problem would certainly provide steady-state solution results with numbers different than those given in Tables 4 and 5, for instance. However, the values of  $R_{\text{H/D}}^{\text{MAR}}$  and  $R_{\text{H/D}}^{\text{MAD}}$  of Table 3 will not be changed significantly since the rates of processes determining  $R_{\text{H/D}}^{\text{MAR}}$  and  $R_{\text{H/D}}^{\text{MAD}}$  are the largest ones. This can be also shown from a perturbative treatment of rate equations. Another limitation of our treatment of the problem was the requirement that electron density is smaller than  $\sim 5 \times 10^{14} \text{ cm}^{-3}$ . This constrain has served to decouple the rate equations with respect to principal quantum number  $n$  of MAR products  $\text{H}^*(n)$  and  $\text{D}^*(n)$ . It is obvious that this constrain can easily be removed; the price for that is a necessity of solving an  $n - n'$  coupled system of rate equations for both MAR and MAD kinetics with  $n, n' = 1 - 5$  and some effective rates for the processes involving the  $n, n' \geq 6$  states. This is, of course, quite feasible in a numerical treatment of coupled rate equations, and the required cross section (rate coefficient) database is available. In a similar way one could include also the full  $v - v'$  kinetics in a numerical treatment of MAR and MAD rate equations, but the problem then will arise with availability of the necessary cross section information for all  $v - v'$  resolved processes involved in the kinetics.

The present treatment of isotope effect problem due to MAR and MAD processes in a two-isotope divertor plasma also neglects the plasma and neutral particle transport in the divertor (except for the account of finite ion residence time, Section 4). The influence of plasma and neutral particle transport on MAR and MAD isotope effects cannot be qualified *a priori*; it

## 6 Concluding Remarks

---

needs to be investigated for a more specific definition of divertor plasma conditions and is, perhaps, outside the validity range zero dimensional plasma chemistry (reaction) kinetics. It is, however, clear that as long as the characteristic timescales for plasma and neutral particle transport effects are longer than the timescales on which MAR and MAD mechanisms operate, the isotope effects produced by these mechanisms will manifest themselves.

The results on  $R_{\text{H/D}}^{\text{MAR}}$  and  $R_{\text{H/D}}^{\text{MAD}}$  given in Table 3 were obtained under the assumption that the population of vibrational states of molecules have a Boltzmann distribution. If this distribution is non-Boltzmann, and favors, for instance, the population of higher  $v$ -states, then the  $R_{\text{H/D}}^{\text{MAR}}$  and  $R_{\text{H/D}}^{\text{MAD}}$  values will be somewhat reduced (due to the fact that the isotope effect in DA process is less expressed for the high- $v$  levels). It should be also mentioned that  $R_{\text{H/D}}^{\text{MAR}}$  and  $R_{\text{H/D}}^{\text{MAD}}$  are sensitive to the values of  $S_{j,\text{H}_2}^\lambda$  and  $S_{j,\text{D}_2}^\lambda$  ( $\lambda=\text{da, ic, cx}$ ), but not much on the values of  $S_{j,\text{HD}}^\lambda$ ,  $\omega_\chi$ ,  $\omega_\eta$ ,  $\xi$  and  $\zeta$ . which appear symmetrically in the nominators and denominators of  $R_{\text{H/D}}^{\text{MAR}}$ ,  $R_{\text{H/D}}^{\text{MAD}}$  ratios. Therefore, for the accurate values of  $R_{\text{H/D}}^{\text{MAR}}$  and  $R_{\text{H/D}}^{\text{MAD}}$  critical is the accuracy of  $S_{j,\text{H}_2}^\lambda$  and  $S_{j,\text{D}_2}^\lambda$  ( $\lambda=\text{da, ic, cx}$ ) only. The rate coefficient data we have used to determine  $S_{j,\text{H}_2}^\lambda$  and  $S_{j,\text{D}_2}^\lambda$  and calculate  $R_{\text{H/D}}^{\text{MAR}}$ ,  $R_{\text{H/D}}^{\text{MAD}}$  in the present work can be considered quite reliable.

The MAR and CX-MAD act as isotope ion charge separation mechanisms, preferring the  $(\text{H}^+) \rightarrow [\text{D}^+]$  and  $(\text{D}^+) \rightarrow [\text{H}^+]$  “conversion”, respectively. For  $T = 1\text{--}3$  eV, the ion charge separation effect of CX-MAD is stronger than that of MAR. The lack of accurate rate coefficients data for reactions 20, 22, 30 and 32 of Table 1 prevents us to make an accurate estimate of the ion charge separation effects of these direct ion-conversion reactions. The entire ion charge separation problem due to MAR and MAD processes remains, therefore, unresolved at present.

Finally, we note that for a D/T plasma with the same parameters as the H/D plasma studied here, the MAR and MAD isotope effects are expected to be smaller than in the H/D case. As we have seen in Section 3, the averaged rate coefficients  $S_{j,\text{AB}}^{\text{da}}$  depend on the reduced mass  $\mu$  of AB molecule as  $\mu^{-1/2}$ . This gives  $S_{j,\text{D}_2}^{\text{da}}/S_{j,\text{T}_2}^{\text{da}} \simeq (\frac{2}{3})^{1/2}$ , which is by a factor of  $\sqrt{3}$  smaller than  $S_{j,\text{H}_2}^{\text{da}}/S_{j,\text{D}_2}^{\text{da}}$ . The physical reason for the inequality  $S_{j,\text{D}_2}^{\text{da}} < S_{j,\text{H}_2}^{\text{da}}$  (or  $S_{j,\text{T}_2}^{\text{da}} < S_{j,\text{D}_2}^{\text{da}}$ ) is that the number of vibrational levels in the heavier molecule

## 6 Concluding Remarks

---

is larger than that number in the lighter molecule. This leads to a smaller population of high- $v$  levels, which provide the main contribution to  $S_{j,AB}^{da}$  and for which the isotope effect is less expressed. Due to the same reason,  $S_{j,D_2}^{ic} < S_{j,H_2}^{ic}$  (or  $S_{j,T_2}^{ic} < S_{j,D_2}^{ic}$ ). Preliminary calculations of  $R_{D/T}^{MAR}$  and  $R_{D/T}^{MAD}$  have shown that for the same plasma parameters and plasma neutral composition, the values of  $R_{D/T}^{MAR}$  and  $R_{D/T}^{MAD}$  are smaller than  $R_{H/D}^{MAR}$  and  $R_{H/D}^{MAD}$  by a factor 2 and 1.5, respectively.

## 7 Tables

A. Negative Ion MAR/MAD	B. Ion-conversion MAR/MAD
1. $e + H_2 \rightarrow H^- + \underline{H}$	14. $H^+ + H_2 \rightarrow \underline{H} + H_2^+$
2. $H^+ + H^- \rightarrow H + H^*(n)$	15. $e + H_2^+ \rightarrow H + H^*(n)$
3. $e + D_2 \rightarrow D^- + \underline{D}$	16. $D^+ + D_2 \rightarrow \underline{D} + D_2^+$
4. $D^+ + D^- \rightarrow D + D^*(n)$	17. $e + D_2^+ \rightarrow D + D^*(n)$
5. $H^+ + D^- \rightarrow H^*(n) + D$	18. $H^+ + D_2 \rightarrow \underline{H} + D_2^+$
6. $D^+ + H^- \rightarrow D^*(n) + H$	19. $D^+ + H_2 \rightarrow \underline{D} + H_2^+$
7. $e + H^*(n) \rightarrow e + H^+ + e$	20. $H^+ + D_2 \rightarrow HD + D^+$
8. $e + D^*(n) \rightarrow e + D^+ + e$	21. $H^+ + D_2 \rightarrow HD^+ + D$
9. $H^+ + D^*(n) \rightarrow H^*(n' \neq n) + D^+$	22. $D^+ + H_2 \rightarrow HD + H^+$
10. $D^+ + H^*(n) \rightarrow D^*(n' \neq n) + H^+$	23. $D^+ + H_2 \rightarrow HD^+ + H$
11. $e + H^- \rightarrow e + \underline{H} + e$	24. $H^+ + HD \rightarrow \underline{H} + HD^+$
12. $e + D^- \rightarrow e + \underline{D} + e$	25. $D^+ + HD \rightarrow \underline{D} + HD^+$
13a. $e + HD \rightarrow H^- + \underline{D}$	26a. $e + HD^+ \rightarrow H^*(n) + D$
13b. $e + HD \rightarrow D^- + \underline{H}$	26b. $e + HD^+ \rightarrow D^*(n) + H$
	27. $e + H_2^+ \rightarrow e + H^+ + \underline{H}$
<b>C. Common Reactions</b>	28. $e + D_2^+ \rightarrow e + D^+ + \underline{D}$
34. $H^*(n) \rightarrow H^*(n' < n) + h\nu$	29a. $e + HD^+ \rightarrow e + H^+ + \underline{D}$
35. $D^*(n) \rightarrow D^*(n' < n) + h\nu$	29b. $e + HD^+ \rightarrow e + D^+ + \underline{H}$
36. $e + H^*(n) \rightarrow e + H^*(n' \neq n)$	30. $H^+ + HD \rightarrow H_2 + D^+$
37. $e + D^*(n) \rightarrow e + D^*(n' \neq n)$	31. $H^+ + HD \rightarrow H_2^+ + D$
38. $e + \underline{H} \rightarrow e + H^+ + e$	32. $D^+ + HD \rightarrow D_2 + H^+$
39. $e + \underline{D} \rightarrow e + D^+ + e$	33. $D^+ + HD \rightarrow D_2^+ + H$

Table 1: Reaction in H<sub>2</sub>/D<sub>2</sub> MAR and MAD kinetics

$S_{j,AB}^\lambda$	T = 1 eV	T = 2 eV	T = 3 eV	Ref.
$\zeta$	0.811	0.629	0.585	[11],[26]
$\xi$	0.19	0.37	0.415	[11],[26]
$\omega_\chi$	1.01	0.91	0.70	[11]
$\omega_\eta$	0.993	1.023	1.053	[11],[26]
$S_{1,H_2}^{da}$	6.65	12.96	11.54	[12]
$S_{3,D_2}^{da}$	4.72	9.034	7.83	[12]
$S_{13,HD}^{da}$	5.85	11.03	9.74	[12]
$S_{14,H_2}^{ic}$	10.98	28.60	39.605	[13]
$S_{16,D_2}^{ic}$	10.48	27.12	38.08	[13],(a)
$S_{24,HD}^{cx}$	8.77	24.58	36.23	[13],(a)
$S_{19,H_2}^{cx}$	9.61	26.31	37.82	[13]
$S_{18,D_2}^{cx}$	9.10	24.95	36.37	(a)

**Table 2:** Values of  $\omega_\chi$ ,  $\omega_\eta$ ,  $\xi$ ,  $\zeta$  and  $S_{j,AB}^\lambda$  (units of  $10^{-10}$  cm<sup>3</sup>/s) for T=1,2 and 3 eV. Note (a): see text

$[\mathbf{H_2}] : [\mathbf{D_2}] : [\mathbf{HD}]$	$\mathbf{T = 1\ eV}$	$\mathbf{T = 2\ eV}$	$\mathbf{T = 3\ eV}$
1:1:0 MAR	1.032	1.040	1.035
1:1:0 MAD	1.137	1.128	1.099
1:1:0.5 MAR	1.026	1.032	1.030
1:1:0.5 MAD	1.110	1.102	1.079
1:1:1 MAR	1.022	1.027	1.023
1:1:1 MAD	1.091	1.110	1.066
1:1:2 MAR	1.017	1.020	1.017
1:1:2 MAD	1.069	1.064	1.049
1:1:6 MAR	1.008	1.010	1.008
1:1:6 MAD	1.034	1.032	1.024

**Table 3:** Values of  $R_{\text{HD}}^{\text{MAR}}$  and  $R_{\text{HD}}^{\text{MAD}}$  for various molecular neutrals compositions and  $T = 1, 2, 3\text{ eV}$

<b>T</b>	<b>2 eV</b>	<b>3 eV</b>
$n_0(10^{14} \text{ cm}^{-3})$	0.66	14.9
1:1:0	1.026	1.670
1:1:0.5	1.021	1.553
1:1:1	1.018	1.403
1:1:2	1.013	1.286
$n_0(3 \times 10^{14} \text{ cm}^{-3})$	3.29	64.6
1:1:0	1.138	9.23
1:1:0.5	1.109	6.75
1:1:1	1.092	4.34
1:1:2	1.067	2.97

**Table 4:** Overall MAR isotope effect,  $r_0^{\text{MAR}}$ , during the ion residence time for  $T = 2$  and  $3$  eV,  $[e] = 10^{14}$  and  $3 \times 10^{14} \text{ cm}^{-3}$ ,  $L = 10$  m, and different  $[\text{H}_2]:[\text{D}_2]:[\text{HD}]$  ratios.

<b>T</b>	<b>2 eV</b>	<b>3 eV</b>
$n_0(10^{14} \text{ cm}^{-3})$	0.66	14.9
1:1:0	1.083	4.08
1:1:0.5	1.066	3.10
1:1:1	1.056	2.59
1:1:2	1.042	2.04
$n_0(3 \times 10^{14} \text{ cm}^{-3})$	3.29	64.6
1:1:0	1.486	$4.45 \times 10^2$
1:1:0.5	1.377	$1.36 \times 10^2$
1:1:1	1.312	$6.21 \times 10^1$
1:1:2	1.226	$2.20 \times 10^1$

**Table 5:** Overall MAD isotope effect,  $r_0^{\text{MAD}}$ , during ion residence time for  $T = 2$  and  $3$  eV,  $[e] = 10^{14}$  and  $3 \times 10^{14} \text{ cm}^{-3}$ ,  $L = 10$  m, and different  $[\text{H}_2]:[\text{D}_2]:[\text{HD}]$  ratios.



## References

- [1] M. Bessenroth-Weberpals, F. Wagner and the ASDEX Team, Nucl. Fusion 33, No. 8, 1205 (1993).
- [2] M.Z. Tokar, D. Kalupin and B. Unterberg, Phys. Rev. Lett. 92, No. 21, 215001 (2004).
- [3] M.Z. Tokar, J. Nucl. Mater. 162-164, 648 (1989).
- [4] R.D. Hazeltine, M.D. Calvin, P.M. Valanju et al., Nucl. Fusion 32, No. 1, p3-14 (1992).
- [5] M.G. Holliday, J.T. Muckerman, and L. Friedman, J. Chemical Physics, 54, No. 3, 1058 (1971).
- [6] A.K. Kukushin, S.I. Krashenninnikov, A.A. Pshenov, D. Reiter, Nucl. Materials and Energy, (2017),<http://dx.doi.org/10.1016/j.nme.2016.12.030>
- [7] R.K. Janev, D.E. Post, W.D. Langer et al., J. Nucl. Mater. 121, 10 (1984).
- [8] S.I. Krashenninnikov, A.Yu. Piagrov, and D.J. Sigmar, Phys. Lett. A214, 295 (1996).
- [9] N. Ohno, N. Ezumi, S. Takamura et al., Phys. Rev. Lett. 81, 818 (1998).
- [10] U. Fantz, D. Reiter, B. Heger, D. Coster, J. Nucl. Mater. 290-293 (2001), 367
- [11] R.K. Janev, W.D. Langer, K. Evans and D.E. Post, “Elementary Processes in Hydrogen-Helium Plasmas”, (Springer-Verlag, Berlin, 1987).
- [12] I.I. Fabrikant, J.M. Wadebra and Y. Xu, Physica Scripta, T96, 45, (2002); I.I. Fabrikant and Y. Xu (private communication, 2002).
- [13] A. Ichihara, O. Iwamoto and R.K. Janev, J. Phys. B: At. Mol. Opt. Phys. 32, 4747 (2000).

## REFERENCES

---

- [14] J.A. Terry et al. Phys. Plasmas 5, 1759 (1998); A. Allen, A. Bozek, N. Brooks et al., Plasma Phys. Contr. Fusion 37, A 191 (1995).
- [15] D. Reiter, C. May, M. Baelmans, P. Boerner, J. Nucl. Materials, 241-243, (1997), 342
- [16] D. Rapp, T.E. Sharp and D.D. Briglia, Phys. Rev. Lett. 14, 533 (1965).
- [17] G.J. Schulz and R.K. Asundi, Phys. Rev. 158, 2 (1967); M. Allen and S. Wong, Phys. Rev. Lett. 41, 1795 (1978).
- [18] J.M. Wadehra and J.N. Bardsley, Phys. Rev. Lett. 41, 1795 (1979).
- [19] J.M. Wadehra, Appl. Phys. Lett. 35, 917 (1979).
- [20] Yu.N. Demkov, Phys. Lett. A15, 235 (1965).
- [21] P.S. Krstic, D.R. Schultz and R.K. Janev, Physica Scripta, T96, 61 (2002).
- [22] G. Gioumousis and D.P. Stevenson, J.Chem.Phys. 29, 294 (1958).
- [23] F. Linder, R.K. Janev and J. Botero, in: "Atomic and Molecular Processes in Fusion Edge Plasmas", ed. R.K. Janev (Plenum Press, New York, 1995), p. 397.
- [24] J.G. Wang and P.C. Stancil, Physica Scripta T96, 72 (2002).
- [25] R. Celiberto, R.K. Janev, A. Laricchiuta et al., ADNDT 77, 161 (2001).
- [26] H. Takagi, Physica Scripta T96, 52 (2002).
- [27] R. Celiberto, M. Capitelli and R.K. Janev, Chem. Phys. Lett. 256, 575 (1996); R.Celiberto, A. Laricchiuta, U.T. Lamanna et al., Phys. Rev. A60, 2001 (1999).
- [28] A. Ichihara, O. Iwamoto, K. Yokohama, Atomic and Plasma-Material Interaction Data for Fusion, Vol 9, 193 (2001), International Atomic Energy Agency, Vienna, Austria, ed.: R. Clark



**Jül-4411 • Juni 2018**  
**ISSN 0944-2952**

Mitglied der Helmholtz-Gemeinschaft

